

# Unusual Hall Effect Anomaly in MnSi Under Pressure

Minhyea Lee<sup>1†</sup>, W. Kang<sup>2</sup>, Y. Onose<sup>1</sup>, Y. Tokura<sup>3,4</sup> and N. P. Ong<sup>1</sup>

<sup>1</sup>*Department of Physics, Princeton University, Princeton, NJ 08544, USA*

<sup>2</sup>*Department of Physics, University of Chicago, Chicago, IL 60637, USA*

<sup>3</sup>*Department of Applied Physics, University of Tokyo, Tokyo 113-8656,*

*Japan* <sup>4</sup>*ERATO, JST, Spin Superstructure Project (SSS), Tsukuba 305-8562, Japan*

(Dated: November 20, 2008)

We report the observation of a highly unusual Hall current in the MnSi in an applied pressure  $P = 6\text{--}12$  kbars. The Hall conductivity displays a distinctive step-wise field profile quite unlike any other Hall response observed in solids. We identify the origin of this Hall current with the effective real-space magnetic field due to chiral spin textures, which may be a precursor of the partial-order state at  $P > 14.6$  kbar. We discuss evidence favouring the chiral spin mechanism for the origin of the observed Hall anomaly.

In the non-centrosymmetric helical magnet MnSi, a novel magnetic state with “partial order” has been reported by Pfleiderer and coworkers above a critical applied pressure  $P_c = 14.6$  kbar [1, 2, 3]. The neutron diffraction intensity is broadly distributed over the surface of a sphere in momentum space, but is resolution limited in the radial direction. Several groups have proposed that the state harbors non-trivial topological spin textures [4, 5, 6, 7]. We have observed a highly unusual Hall current in MnSi at pressures (6–12 kbar) just below  $P_c$ , which appears to be caused by fluctuations into the chiral spin state at temperatures  $T$  near the Curie transition temperature  $T_C$ .

At ambient pressure, MnSi undergoes a transition at  $T_C \simeq 30$  K to a helical state with a long pitch  $\lambda \sim 180$  Å with its wavevector  $\mathbf{q}$  weakly pinned along the  $\langle 111 \rangle$  direction, consistent with its cubic B20 symmetry. In a magnetic field  $\mathbf{H}$ ,  $\mathbf{q}$  shifts to alignment, and the helical state evolves to a conical magnetic state, whose cone angle steadily decreases to zero at a field  $H_s \sim 0.6$  T. Under pressure,  $T_C$  decreases monotonically, reaching zero at the critical pressure  $P_c \sim 14.6$  kbar (Fig. 1, inset). Above  $P_c$ , the “partial-order” state displays a non-Fermi liquid exponent in its resistivity in addition to the unusual neutron diffraction spectrum. The new Hall anomaly is observed in weak  $H$  in the pressure interval  $6 < P < 12$  kbar below the curve of  $T_c$  vs.  $P$  (shaded region in the inset of Fig. 1). Main panel of Fig. 1 displays the Hall resistivity  $\rho_{yx}$  measured at several temperatures ( $T$ ) with  $P$  fixed at 11.4 kbar ( $T_C = 11.3$  K). At the lowest  $T$  (0.35 and 2.5 K),  $\rho_{yx}$  is hole-like and  $H$ -linear. At 5 K, a prominent anomaly appears in a narrow field interval between  $H_1 \sim 0.1$  T and  $H_2 \sim 0.45$  T. Significantly, it exists only below the field  $H_s \sim 0.6$  T at which the cone angle closes. At such low fields, the Hall anomaly corresponds to a very large Hall current, as discussed below. As  $T$  increases towards  $T_C$ , the anomaly remains clearly distinct from a growing broad background that persists to fields above 7 T. The background is the *conventional* anomalous Hall effect (AHE) term common to all ferromagnets. Hence, in addition to being qualitatively distinct from the familiar AHE term, the anomaly displays a field profile quite unlike any previously reported in bulk conductors

(either magnetic or non-magnetic).

Motivated by the results of Refs. [1, 2, 3], several groups [4, 5, 6, 7] have proposed states comprised of crystalline arrays of magnetic textures. In Ref. [4], the transition at  $P_c$  is from a single-spiral state to a bcc “spin crystal” comprised of 6 spirals. In Refs. [5, 7], the proposed state is either a square lattice configuration of skyrmions [5, 7], or a cubic network of line defects which are double-twist configurations [7]. The textures are closely related to the defects previously studied in the blue phase of nematic liquid crystals [6, 7].

Hall measurements were made in a <sup>3</sup>He cryostat using a miniature clamp-type pressure cell (13 mm dia.) made of BeCu alloy and tungsten carbide with Fluorinert (FC-77) as the pressure medium. At low  $T$ , the pressure was calibrated by the superconducting transition of a Pb coil detected by AC susceptibility. The high-purity MnSi crystals (of resistivity ratio  $\rho(300\text{K})/\rho(4.2\text{K}) \simeq 60$  and of size  $\sim 1.1\text{ mm} \times 0.5\text{ mm} \times 60\ \mu\text{m}$ ) were grown in a floating-zone furnace. Because of the unusual nature of the Hall anomaly, we adopted several precautions to eliminate spurious causes. The Hall voltage  $V_H$ , measured by both DC and AC lock-in techniques, was checked to scale linearly with current  $I$  (typically 0.5 to 1 mA). At each  $T$  and  $P$ ,  $V_H$  was recorded with  $H$  swept in the sequence  $0 \rightarrow -1T \rightarrow 0 \rightarrow 1T \rightarrow 0$  to eliminate errors from weak, induced emf’s and drifts in  $T$ . The observed Hall anomaly is always antisymmetric in  $H$  even without antisymmetrization of the 4 raw curves. As the signal-to-noise ratio increased with improved temperature regulation ( $\delta T \sim 50$  mK) and reduction of the field sweep rate (to 0.02 T/min.), we observed the Hall anomaly to become better resolved. Results obtained in the 2 crystals investigated are closely similar.

In ferromagnets, the observed Hall resistivity  $\rho_{yx}$  is the sum of the ordinary Hall resistivity  $\rho_{yx}^N = \sigma_{xy}^N \rho^2$  and the AHE term  $\rho_{yx}^A = \sigma_{xy}^A \rho^2$ , where  $\rho = \rho_{xx}$  is the resistivity and  $\sigma_{xy}^N$  and  $\sigma_{xy}^A$  are the ordinary and anomalous Hall conductivities, respectively. Dividing by  $\rho^2$ , we have

$$\frac{\rho_{yx}}{\rho^2} = \sigma_{xy}^N + \sigma_{xy}^A. \quad (1)$$

The first term is strictly  $H$  linear in low  $H$ , while the sec-

ond term scales as the uniform magnetization  $M(T, H)$ .

To bring out the surprising nature of the new anomaly, we first review the Hall Effect in MnSi at ambient  $P$  [8, 9]. In high-purity MnSi, the long electron mean-free-path  $\ell$  produces a very large magnetoresistance (MR) below  $T_C$ . Lee *et al.* [9] have shown that, in spite of the large MR, the  $H$  dependence of  $\sigma_{xy}^A$  at ambient  $P$  strictly mimics that of  $M(T, H)$ , viz.  $\sigma_{xy}^A(T, H) = S_H M(T, H)$ , with  $S_H$  a constant independent of  $T$  and  $H$ . This scaling confirms a key prediction of the Karplus-Luttinger (KL) theory [10] (and its modern extensions [11, 12, 13]).

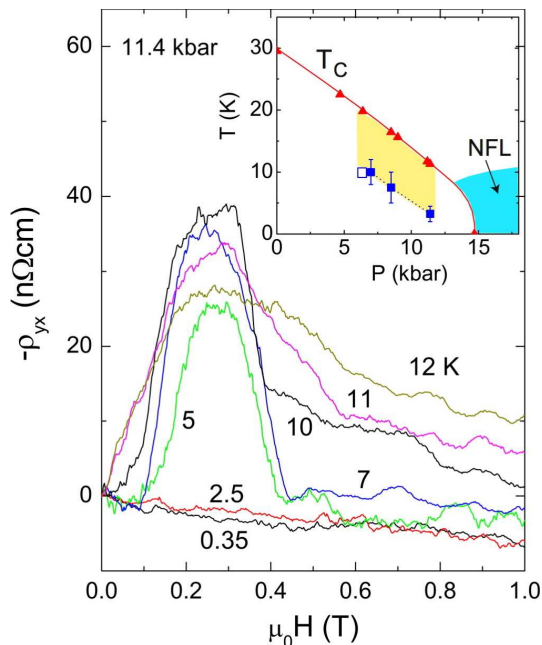


FIG. 1: (color online) (Main panel) Curves of  $-\rho_{yx}$  in MnSi at 11.4 kbar revealing a large Hall anomaly in the field range  $0.1 < H < 0.45$  T for several  $T < T_C$  ( $T_C = 11.3$  K), with  $\mathbf{H}$  nominally along (111). The anomaly (electron-like in sign) arises from a new contribution  $\sigma_{xy}^C$  to the total Hall conductivity. In the phase diagram (inset), the shaded region is where  $\sigma_{xy}^C$  is resolved.  $T_C$  was determined from  $\rho$  vs.  $T$ . Data from Samples 1 and 2 are shown as solid and open squares, respectively. The non-Fermi liquid (NFL) region is shaded blue (adapted from Ref. [2]).

Returning to the Hall curves in MnSi under pressure, we plot in Fig. 2 curves of  $\rho_{yx}$  over a broader field range, with  $P$  fixed at 8.5 kbar (at which  $T_C = 16.4$  K). Starting at 5 K, we observe that  $\rho_{yx}$  is linear in  $H$  to 7 T. This reflects the dominance of  $\sigma_{xy}^N \sim \ell^2$  in the limit of large  $\ell$ . With increasing  $T$ , however, the rapid increase of  $\rho$  strongly amplifies the anomalous term  $\rho_{yx}^A$  which emerges as a negative contribution with a broad shoulder (e.g. at 2.5 T at 25 K). We refer to this term as the “conventional” AHE term. At 10 and 15 K, we see the emergence of the new Hall anomaly as a sharp negative spike in weak fields. Raising  $T$  above  $T_C$  removes the spike (curves at 20 and 25 K). The curves above  $T_C$  are closely similar to those observed at ambient  $P$  (where the

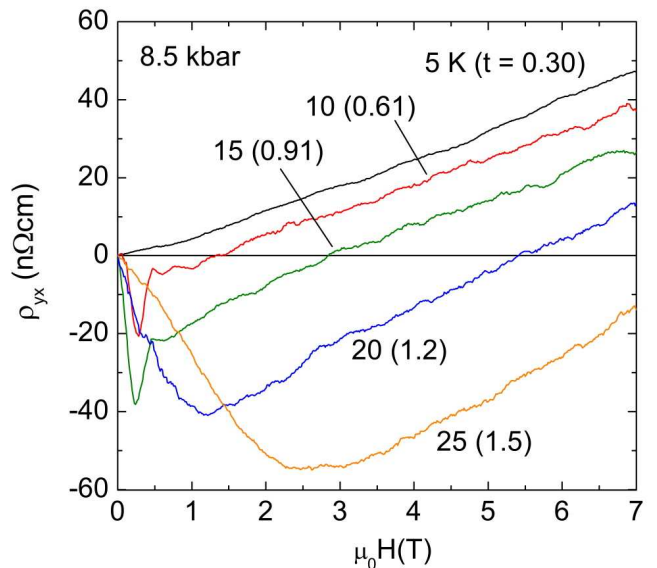


FIG. 2: (color online) Curves of  $\rho_{yx}$  extending to 7 T showing the relation of the Hall anomaly to other Hall terms (at the applied  $P = 8.5$  kbar,  $T_C = 16.4$  K). At 5 K, the hole-like  $\sigma_{xy}^N$  dominates  $\rho_{yx}$  to produce an  $H$ -linear background. At  $T = 10$  and 15 K, at which the Hall anomaly is observed as sharp negative spikes, the AHC term  $\rho_{yx}^A = \sigma_{xy}^A \rho^2$  grows in prominence as  $\rho$  increases. Above  $T_C$  (20 and 25 K), the Hall anomaly vanishes, while  $\rho_{yx}^A$  continues to increase in magnitude. The reduced temperature  $t = T/T_C$  is shown in parenthesis for each curve.

spike is absent).

The new Hall anomaly represents a third contribution to the total Hall current. Recent research has shown that a new Hall current can arise in magnetic systems from the interaction between the spin of the carrier and textures in  $\mathbf{M}(\mathbf{r})$ . We compare our findings with this spin-mediated mechanism using reasonings based on the Berry phase.

In the past decade, the Berry-phase approach has greatly extended the purview of the KL theory [11, 12, 13]. In a periodic lattice, the “overlap” of wave functions  $u_{\mathbf{k}}$  defines the Berry gauge potential  $\mathbf{A}(\mathbf{k}) = \langle u_{\mathbf{k}} | i \nabla_{\mathbf{k}} | u_{\mathbf{k}} \rangle$ , whose curl gives an effective magnetic field  $\mathbf{\Omega}(\mathbf{k})$  that lives in  $\mathbf{k}$  space. When  $\mathbf{\Omega}(\mathbf{k})$  is rendered finite (by breaking time-reversal invariance), it bends the electron trajectory in  $\mathbf{k}$  space to reproduce the KL term  $\sigma_{xy}^A$  in Eq. 1.

Quite distinct from this strictly orbital coupling, the Berry phase can produce an *additional* effective magnetic field  $\mathbf{B}_\phi$  via the spin degrees of freedom. The spin-mediated mechanism was initially invoked to explain AHE experiments in manganites [14] and pyrochlores [15]. We consider the simplest example in which the spin  $\mathbf{s}$  of a hopping electron aligns by Hund coupling  $J_H$  to the ion’s local moment  $\mathbf{S}_i$  at a site  $i$  [14, 15]. As the electron completes a closed loop linking 3 non-coplanar spins  $\mathbf{S}_i$  ( $i = 1, 2, 3$ ),  $\mathbf{s}$  describes a cone of finite solid angle  $\Omega$  (Fig. 3, inset). Hence, the electron ac-

quires a Berry phase  $\phi_B = \frac{1}{2}\Omega$ , which translates to a magnetic field in real space  $\vec{B}_\phi = (\phi_B/2\pi)(\phi_0/\mathcal{A})$  that can be extremely large ( $\mathcal{A}$  is the loop area and  $\phi_0$  the flux quantum). For e.g., even for  $\Omega \sim \pi/100$  over an area  $\mathcal{A} \sim 5 \times 5 \text{ \AA}^2$ , we have  $B_\phi \sim 42 \text{ T}$ . In turn,  $\mathbf{B}_\phi$  produces a large Hall conductivity  $\sigma_H^C$  that is proportional to the chirality  $\chi_c = \mathbf{S}_1 \cdot \mathbf{S}_2 \times \mathbf{S}_3$  [15, 16, 17, 18].

The foregoing also applies to itinerant ferromagnets. In a spiral helimagnet such as MnSi, the local spin direction  $\mathbf{S}(\mathbf{r})$  varies periodically with a pitch set by the wavevector  $\mathbf{q}$ . For an itinerant electron, the exchange energy forces its spin  $\mathbf{s}$  to follow the spatial variation of  $\mathbf{S}(\mathbf{r})$ . However, as emphasized in Ref. [19], a spiral state with a single  $\mathbf{q}$  has zero chirality. In order to produce finite chirality, we must have a multi- $\mathbf{q}$  spiral state, as has been proposed for the partial order state for  $P > P_c$ .

In the novel states proposed [4, 5, 6, 7], the presence of skyrmions or double-twist configurations naturally leads to chirality. We expect  $\sigma_H^C$  to be proportional to the skyrmion number  $N_s = \int d^3r \Phi_z(\mathbf{r})$ , with the skyrmion density  $\Phi_z = (8\pi)^{-1} \hat{\mathbf{n}} \cdot (\partial_x \hat{\mathbf{n}} \times \partial_y \hat{\mathbf{n}})$  and  $\hat{\mathbf{n}} = \mathbf{S}(\mathbf{r})/|\mathbf{S}(\mathbf{r})|$ .

For the region of our Hall experiment ( $P < P_c$ ), we expect fluctuations towards the multi- $\mathbf{q}$  state to be favorable at temperatures just below  $T_C$  (the fluctuations are strongly suppressed as  $T \rightarrow 0$ ). Hence, within the broad swath in which  $\sigma_{xy}^C$  is observed (Fig. 1 inset), we propose that chirality exists caused by strong fluctuations into multi- $\mathbf{q}$  helical states.

There is considerable evidence for strong fluctuations in the region  $P < P_c$ . The muon spin rotation data by Uemura *et al.* [20] show that, for  $P < P_c$ , magnetic order exists only in a partial volume fraction, in agreement with conclusions from nuclear magnetic resonance [21] and neutron scattering [22] experiments. In a broad range of  $P$  below  $P_c$ , strong fluctuations appear as a precursor to the partial-ordered state above  $P_c$ .

Within this picture, we may understand several puzzling features of the Hall data (as well as the MR). To examine these issues in more detail, we transform  $\rho_{yx}$  to  $\sigma_{xy} = \rho_{yx}/\rho^2$  using the simultaneously measured curve of  $\rho$  vs.  $H$ . As plotted in Fig. 3a, the Hall anomaly is now apparent as a large Hall conductivity  $\sigma_{xy}^C$ , with a distinctive field profile. Just below  $T_C$ , the anomaly first appears as a shallow hull feature (compare curves at 12 and 11 K). With decreasing  $T$ , it deepens considerably. Comparing the curves of  $\sigma_{xy}$  with the MR curves, we see that  $\sigma_{xy}^C$  is restricted to the narrow interval  $H_1 < H < H_2$ . At 5 K, its magnitude is  $\sim 10$  times larger than the other 2 Hall terms, and  $\sim 1\%$  of the zero- $H$  conductivity  $\sigma$ . Finally, at 2.5 K, the anomaly vanishes, leaving an  $H$ -linear background that is dominated by  $\sigma_{xy}^N$ .

We now discuss the evidence that we believe provide strong arguments for the chiral-spin mechanism. First, we note that, between  $H_1$  and  $H_2$ ,  $|\sigma_{xy}^C|$  attains remarkably large values. At ambient pressure 5 K with  $H = 0.3 \text{ T}$ , the measured values of the ordinary term and the KL term,  $\sigma_{xy}^N$  and  $\sigma_{xy}^A$ , are  $\sim +3.2 \times 10^4$  and  $-1.2 \times 10^4$   $(\Omega\text{m})^{-1}$ , respectively [9]. By comparison,  $|\sigma_{xy}^C|$  is 10

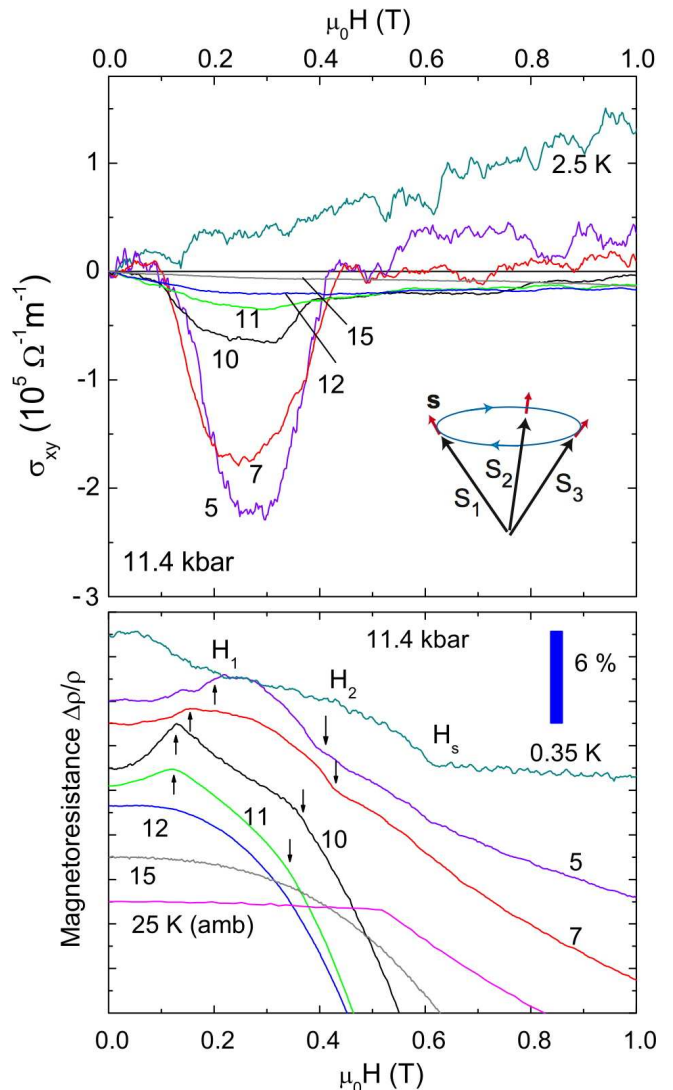


FIG. 3: (color online) Panel (a) Curves of  $\sigma_{xy}$  vs.  $H$  at  $P = 11.4 \text{ kbar}$  at selected  $T$ . The Hall anomaly  $\sigma_{xy}^C$  is prominent between 11 and 5 K between the fields  $H_1$  and  $H_2$ . At 2.5 K, only the normal term  $\sigma_{xy}^N$  is observed. The inset shows the itinerant spin  $\mathbf{s}$  aligned with the local moment  $\mathbf{S}_i$  on site  $i$  by a large  $J_H$ . As the electron closes the path 1-2-3-1, it acquires a Berry phase  $\phi_B$ . Panel (b) Curves of the MR  $\Delta\rho/\rho$  vs.  $H$  at selected  $T$  at 11.4 kbar (curves are offset for clarity). Below  $T_C$  (11.3 K) anomalies indicate fields  $H_1$  (uparrows),  $H_2$  (downarrows) and  $H_s$ . By comparison, the MR is nearly zero below  $H_s = 0.6 \text{ T}$  at ambient pressure (thin curve at 25 K).

times larger than either of these values. Such a large  $\sigma_{xy}^N$  is difficult to understand with orbital mechanisms given the small values of  $H_1$  and  $H_2$ . However, as discussed above, the chiral spin term is easily capable of producing such a large Hall response. The effective field  $B_\phi$  can easily exceed 40 T despite the small applied  $H$ .

Secondly,  $\sigma_{xy}^C$  is seen to be finite only within a very narrow field interval ( $H_1, H_2$ ). The relatively abrupt vanishing of  $\sigma_{xy}^C$  at  $H_2 \sim 0.45 \text{ T}$  is striking. Such an abrupt

vanishing of the Hall current is extraordinarily difficult to realize with orbital mechanisms (carrier mobilities cannot be abruptly changed in such weak  $H$ ). By contrast, the spin-Berry phase model applied to MnSi anticipates that  $\sigma_{xy}^C$  must vanish at a field below  $H_s$ . As mentioned, the cone angle of the spiral state steadily decreases to zero as  $H \rightarrow H_s \sim 0.6$  T. In the ferromagnetic state above  $H_s$ , spin textures are energetically prohibitive. As the spin textures are removed with increasing  $H$ ,  $\sigma_{xy}^C$  must vanish. Hence  $H_s$  represents an upper bound for a finite  $\sigma_{xy}^C$ . The Hall results show that the vanishing actually occurs at the slightly lower field  $H_2$ .

Thirdly, the picture described also clarifies the origin of the kink anomalies long known in MnSi under pressure. The low- $T$  transverse MR of MnSi is very large and negative throughout its phase diagram because of its long  $\ell$ . Under pressure, weak anomalies appear at fields  $H < H_s$ . Figure 3b compares the transverse MR measured in our sample at ambient pressure and at 11.4 kbar with  $\mathbf{H} \perp \mathbf{I}$  (applied current). First, we examine the MR curve at ambient  $P$  (lowest curve, at 25 K;  $T_C = 30$  K). Surprisingly, the MR is almost zero below  $H_s$ . A sharp kink at  $H_s$  signals saturation of the moments, followed by a steep decrease of  $\rho$  at larger  $H$ . The absence of MR implies that, as  $\mathbf{q}$  re-orient in  $\mathbf{H}$  and the cone

angle decreases, there is no change in the carrier scattering rate  $\Gamma$ . Consequently, the changes below  $H_s$  involve no change in magnetic disorder or the creation of spin defects at ambient  $P$ . The “rigidity” of the spiral state at ambient pressure also explains why the Hall anomaly is not observed at ambient pressure.

By contrast, at  $P = 11.4$  kbar, the MR exhibits kinks in the interval  $0 < H < H_s$ . Above  $T_C$  (11.3 K), the MR decreases smoothly. At 11 K, the 2 field scales  $H_1$  and  $H_2$  inferred from  $\sigma_{xy}$  (Fig. 3b) become apparent (up and down arrows, respectively). Their positions change only slightly with  $T$ . However, they become more sharply defined as  $T$  approaches  $T_C$  from below. Throughout the interval  $(0, H_s)$ , the visible MR anomalies imply that changes in the magnetic structure are accompanied by the production of magnetic defects and textures which change  $\Gamma$ . Hence, in both transport channels, the onset and disappearance of  $\sigma_{xy}^C$  at 11.4 kbar at  $H_1$  and  $H_2$  are nearly coincident with the MR anomalies.

We thank B. Binz, A. Vishwanath and M. Hermele for valuable discussions. The research at Princeton is supported by the U.S. National Science Foundation under MRSEC Grant DMR 0213706.

<sup>†</sup> Present address of ML :National Institute of Standards and Technology, Boulder, CO 80305.

- 
- [1] C. Pfleiderer, S. R. Julien and G. G. Lonzarich, *Nature* **414**, 427- 429 (2001).
- [2] C. Pfleiderer, D. Reznik, L. Pintschovius, H. v. Löhneysen, M. Garst and A. Rosch, *Nature* **442**, 227-231 (2004).
- [3] C. Pfleiderer, P. Böni, T Keller, U.K. Rössler and A. Rosch, *Science* **316**, 1871 (2007).
- [4] B. Binz, A. Vishwanath, and V. Aji, *Phys. Rev. Lett.* **96**, 207202 (2006); B. Binz and A. Vishwanath, *Phys. Rev. B* **74**, 214408 (2006).
- [5] U. K. Rössler, U. N. Bogdanov and C. Pfleiderer, *Nature* **442**, 797- 801 (2006).
- [6] S. Tewari, D. Belitz and T. R. Kirkpatrick, *Phys. Rev. Lett.* **96**, 047207 (2006).
- [7] I. Fischer, N. Shah, and A. Rosch, *Phys. Rev. B* **77**, 024415 (2008).
- [8] N. Manyala, *et al.* *Nature Materials* **3**, 255-262 (2004).
- [9] M. Lee, Y. Onose, Y. Tokura and N. P. Ong, *Phys. Rev. B* **75**, 172403 (2007).
- [10] R. Karplus and J. M. Luttinger, *Phys. Rev.* **95**, 1154 (1954).
- [11] Ganesh Sundaram and Qian Niu, *Phys. Rev. B* **59**, 14915 (1999).
- [12] M. Onoda, N. Nagaosa, *J. Phys. Soc. Jpn.* **71**, 19 (2002).
- [13] T. Jungwirth, Qian Niu, A. H. MacDonald, *Phys. Rev. Lett.* **88**, 207208 (2002).
- [14] P. Matl *et al.*, *Phys. Rev. B* **57**, 10248 (1998).
- [15] Y. Taguchi, Y. Oohara, H. Yoshizawa, N. Nagaosa, Y. Tokura, *Science* **291**, 2573 (2001).
- [16] J. Ye *et al.*, *Phys. Rev. Lett.* **83**, 3737 (1999).
- [17] Gen Tatara and Hikaru Kawamura, *Jnl. Phys. Soc. Jpn.*, **71**, 2613 (2002).
- [18] M. Onoda, G. Tatara and N. Nagaosa, *Jnl. Phys. Soc. Jpn.*, **73**, 2624 (2002).
- [19] B. Binz and A. Vishwanath, *Physica B* **403**, 1336 (2008).
- [20] Y. J. Uemura *et al.*, *Nature Physics* **3**, 29 (2007).
- [21] W. Yu, F. Zamborszky, J.D. Thompson, J. L Sarrao, M.E. Torelli, Z. Fisk and S. E. Brown *Phys. Rev. Lett.* **92** 086403 (2005).
- [22] B. Fåk, R. A. Sadykov, J. Flouquet and G. Lapertot, *J. Phys.:Condens. Matter* **17** 1635-1644 (2005).